

REMOTE SENSING OF THE THERMOPHYSICAL PROPERTIES OF THE MARTIAN SURFACE WITH VISIBLE AND NEAR INFRARED ORBITAL MEASUREMENTS. J. Audouard¹, F. Poulet¹, M. Vincendon¹, J-P. Bibring¹, B. Gondet¹, Y. Langevin¹, ¹Institut d'Astrophysique Spatiale, Université Paris-Sud, Orsay (joachim.audouard@ias.u-psud.fr)

Introduction : The Martian surface temperature is controlled by radiative exchanges with the atmosphere and thermal conduction with the subsurface. The specific thermal behavior of a surface is described by its thermophysical properties : solar albedo and thermal inertia (TI), which is defined as the square root of heat capacity, bulk conductivity and density and expressed in $J.m^{-2}.K^{-1}.s^{-1/2}$. Laboratory thermal inertia retrievals are based on multiple and dynamic measurements, but it is possible to derive a best-fitting thermal inertia from a single orbital temperature measurement using a global climate model to produce reference temperature curves [Kieffer et al., 1977; Mellon et al., 2000 ; Fergason et al, 2006]. Such derived thermal inertia is model-dependent. The most common model assumption is homogeneity (horizontally and vertically) of the surface modeled, leading derived thermal inertia to change with local time and season as the variations of the real thermal cycle are a combination of different subpixel components, or are not reproduced in the model (thin-layered subsurface). Martian surfaces exhibit large apparent thermal inertia variations during the day and year [Putzig and Mellon, 2007a ; 2007b], a behavior that reveals its widespread non-local homogeneity.

We use the OMEGA visible and near infrared spectral dataset (0.36-5.1 μ m) for which new transfer function for the long wavelength detector are available [Jouglet et al., 2008], along with a Global Climate Martian (GCM) modeler developed in collaboration between the Stanford University and the Laboratoire de Météorologie Dynamique [Forget et al., 1999] to investigate the albedo and the thermal inertia of the martian surface. Of special interest is the elliptical orbit of Mars Express, which yield to a novel sampling of the Martian surface thermal cycle at various solar longitude and local time, compared to the TES and THEMIS heliosynchronous datasets.

Parametrization: The main input parameters of the GCM used in this work are summarized in table 1.

Parameter	albedo	local slope and azimuth	Pressure	dust opacity	thermal inertia
obtained by	OMEGA	MOLA	predictor	MERs	free parameter

Table 1. Main input parameters for the GCM

We compute a lambertian solar albedo for each pixel using OMEGA 0.36-2.5 μ m spectral reflectance data, and extending it to 0.25 μ m with a scaled martian composite UV spectra [Bell and Ansty, 2007].

The spectra are corrected from aerosol contribution using lookup tables constructed with a Monte-Carlo statistical model of optical paths as a function of geometry and dust opacity [Vincendon and Langevin, 2010]. Our solar albedo shows good agreement with published TES-derived bolometric albedo maps [Putzig and Mellon, 2007a].

Systematic comparison data/model : We use the same method to correct the contribution of atmospheric dust to the radiance observed at 5 μ m, likely to decrease brightness temperature. OMEGA can monitor surface temperatures larger than about 180K, hence we limit our approach to latitudes lower to 60 degrees and to day times. TI being the only free parameter, we work with the variable $\Delta T = T_{\text{omega}} - T_{\text{model}}$ (K), T_{model} being the output of the model at its set inertia and at OMEGA local time and solar longitude of the acquisition. We have performed a systematic comparison between OMEGA derived temperatures at 5 μ m and surface temperature modeled using the TES dayside apparent thermal inertia seasonal maps (each 10 degrees of solar longitude). The result of the comparison is shown in Figures 1 and 2.

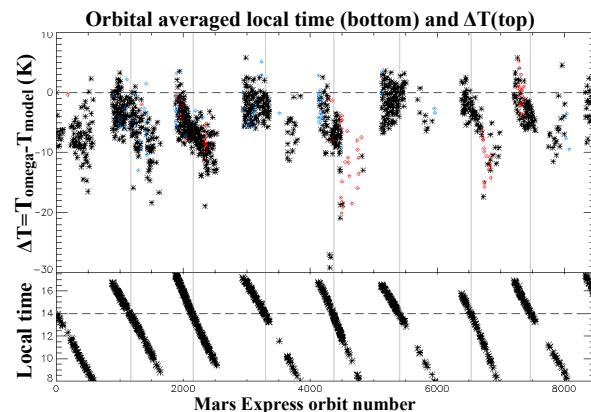


Figure 1. Comparison of surface temperatures derived at 5 μ m from OMEGA data with temperatures modeled with TES 2:00PM seasonal apparent thermal inertia maps [Putzig and Mellon, 2007a]. Every dot is the averaged ΔT of one orbit. Almost 4 full martian years of OMEGA data are represented in this plot. Red dots represent high optical dust opacity orbits.

The ΔT is at first order dominated by the local time of the orbit. A discrepancy is systematically observed between TES-reconstructed and OMEGA-derived temperatures at the same local time and solar longitude. We observe a strong first order dependency of ΔT to local time and a second order dependency to the surface properties.

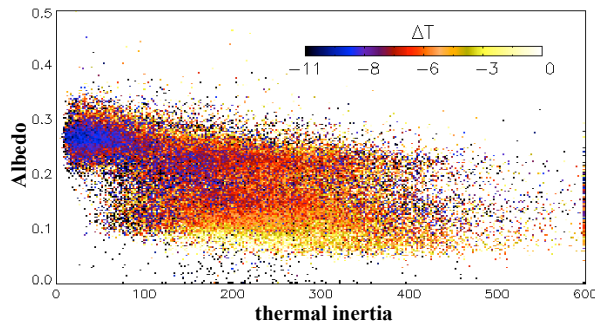


Figure 2. ΔT as a function of solar albedo and TES dayside seasonal apparent thermal inertia. The color represent the averaged ΔT of all the data points used to construct figure 1 corresponding to the albedo and thermal inertia of the bin. The ΔT variations of figure 1 have a second order correlation to the thermophysical properties of the surface.

Heterogeneities : Our GCM allows the user to set two layers of soil, of chosen inertia and first layer depth. It is similar to the work presented by [Mellon and Putzig, 2007], which allows direct comparison between a two layers thermal cycle and an homogeneous thermal cycle.

Effects of horizontal heterogeneities can be also simulated. One can reproduce the thermal cycle of sub-pixel horizontal mixing of two types of material by area-averaging the Stefan-Boltzman's law of the two materials modulated by their emissivity.

We select all optimal OMEGA acquisitions above the Meridiani region and construct a map binned at $0.05^\circ \times 0.05^\circ$ ($\approx 3 \times 3 \text{ km}$ at the equator) between 5°W , 5°S , 5°E and 5°N . Each bin gathers all observations available for its location and their specific parameters. The figure 3 shows the temperature observations for two selected pixels of this map. The first one is represented with black diamonds and belongs to the same geological unit Opportunity landed on as reported in [Arvidson et al., 2003]. We dispose of 8 different acquisitions (hence 8 different local times and solar longitudes) and the apparent thermal inertia has a decreasing trend with local time. The second pixel displayed (orange triangles), the 10 different acquisitions show an increasing trend of apparent thermal inertia with local time. Seasonal trends, of lower amplitudes, are mixed to diurnal trends in this plot.

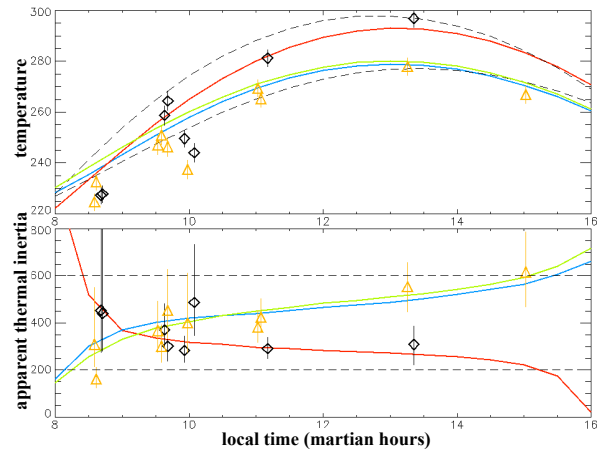


Figure 3. Temperature (top) and Apparent thermal inertia (bottom) as a fonction of local time.

Orange triangles : 4.25°N , 4.4°W

Black diamonds : 2.3°S , 3.15°W

The curves represent different surface temperature modelisations at an arbitrary solar longitude of 200° (top) and apparent thermal inertia derived from them (bottom) :

- **dashed curves (top) and lines (bottom) :** homogeneous modelisation for $TI=200$ and $TI=600$
- **blue curves :** 40% rock at $TI=2500$ mixed with 60% sand at $TI=250$
- **red curves :** 5 millimeters of duricrust-like material at $TI=750$ underlayed by sand at $TI=250$
- **green curves :** 3 millimeters of sand at $TI=250$ underlayed by a duricrust at $TI=650$.

Conclusions : This study indicates : 1) it is possible to retrieve physical properties from NIR OMEGA data ; 2) heterogeneity have to be taken into account in order to model the daytime temperature variation ; 3) simple heterogeneity can reproduce the data ; 4) further work will be to derive global maps of thermal inertia. The thermal cycle of the Martian surface remains nevertheless largely under-sampled, leading to an inevitable non-uniqueness of the heterogeneity solution fitting the observations.

References : Arvidson R.E et al. (2003), *JGR* 108, E12, 8073 ; Bell J. F. and Ansty T. M. (2007) *Icarus* 191, 581–602 ; Fergason R. L. et al., (2006) *JGR* 111, E12004 ; Forget F. et al. (1999), *JGR-Planet* 104, 24,155–24,176 ; Jouglet D. et al. (2008), *Planetary and Space Science* 57, 1032–1042 ; Kieffer, H. H. et al. (1977) *JGR* 82, 4249–4291 ; Mellon M. T. et al. (2000), *Icarus* 148, 437–455 ; Mellon M. T. and Putzig N. E. (2007), *Lunar and Planetary Science XXXVIII*, Abstract 2184 ; Putzig N. E. and Mellon M. T. (2007a), *Icarus* 191, 52–67 ; Putzig N. E. and Mellon M. T. (2007b), *Icarus* 191, 68–94 ; Vincendon M. and Langevin Y. (2010), *Icarus* 207, I. 2, 923–931